Shape Effects on the Structure and Response of the Polymeric Particles Synthesized from Cholesteric Liquid Crystal Templates

Deniz Işınsu Avşar[1] iD **, Emre Büküşoğlu*[2]** iD

*[1,2] Orta Doğu Teknik Üniversitesi Mühendislik Fakültesi Kimya Mühendisliği, ANKARA

Abstract: Liquid crystals (LCs) have been shown to provide molecular templates for the synthesis of polymeric particles. Past studies have revealed the elastic effects to dominate internal configuration of the LC molecular templates for the sizes below 10 μm. Sacrificial microwells were used in this study to study the effect of shapes of the particles synthesized from the cholesteric liquid crystals on their structure and response. Specifically, mixtures of diacrylate based reactive (RM257) and non-reactive mesogens (E7), and chiral dopant (S811) were initially filled into circular, triangular, square and star shaped microwells made from polyvinyl alcohol. After photopolymerization followed by the extraction of the non-reactive part, the particles were obtained. Optical and responsive characterization of the particles showed that the elastic effects of the liquid crystals can also be observed within the particles of the sizes of 50 μm, significantly above the usually expected sizes. We found that the three-dimensional confinement, inhomogeneous surface anchoring and the cholesteric symmetry to play a critical role in the dominant effect of elasticity at larger sizes. The findings of this study will be used in the design of responsive polymeric particles used in the sensing of the vapors of volatile organic compounds.

Kolesterik Sıvı Kristal Şablonları ile Sentezlenmiş Polimerik Parçacıkların Şekillerinin Yapıları ve Tepkileri Üzerine Etkisi

Öz: Sıvı kristal moleküler şablonları polimerik parçacıkların sentezine olanak sağlamaktadır. Geçmiş çalışmalar sıvı kristal elastik etkilerinin 10 μm boyutlarından küçük boyutlardaki parçacıkların içsel organizasyonlarına kritik rol oynadığını göstermiştir. Bu çalışmada mikrokuyucuk yöntemi kullanılarak kolesterik şablonlu sentezlenen parçacıkların şekilleri üzerinde hakimiyet sağlanmış, yapıları ve tepkisellikleri incelenmiştir. Diakrilat gruplu reaktif (RM257) mezojenler, reaktif olmayan (E7) mezojenler ve kiral katkı maddesi (S811) karışımları öncelikle yuvarlak, üçgen, kare ve yıldız şeklindeki polivinil alkol mikrokuyucuklara doldurulmuştur. Fotopolimerizasyon ve takip eden ekstraksiyon sonucunda polimerik parçacıklar elde edilmiştir. Parçacıkların optik ve tepki karakteristikleri incelendiğinde sıvı kristal elastik enerjilerinden kaynaklı düzenlerin 50 μm boyutlarında, daha önceki çalışmalarda gözlemlenen boyutlardan daha büyük boyutlarda, etkili olduğu gözlemlenmiştir. Üç boyutlu sıkıştırılmış ortamın varlığının, homojen olmayan yüzey yöneliminin ve kolesterik düzen simetrisinin bu etkide önemli rol oynadığı bulunmuştur. Bu çalışmanın bulguları sensörler veya tepkisel malzemelerin sentezinde kullanılacak bilgiler içermektedir.

*İlgili Yazar: emrebuk@metu.edu.tr

1. Introduction

Liquid crystals (LCs) are delicate mesophases that exhibit fluidic properties while maintaining a significant degree of molecular ordering.[1] In the nematic phases, the molecules exhibit orientational order parallel to a direction called the director. When a chiral dopant was used with a nematic phase, the chiral twisting of the mesogens result in the formation of the cholesteric liquid crystals (CLCs), which are characterized by a pitch size describing the length of a 2π twist.[1] At high loadings of the chiral dopant, this periodicity results in Bragg reflections of visible light that is critical for optical filtering applications.[2] Liquid crystal displays (LCDs) are one of the most successful application of LCs realized to date that employ their fluidic and ordering properties besides their birefringent optical properties. Beyond displays, LCs are currently being developed for use as sensors, actuators, optical filters, etc. In addition to these applications that employ their dynamic nature, LCs are currently being used for the synthesis of polymeric materials.[3,4]

The properties that distinguish LCs from their isotropic counterparts can be described under three fundamental concepts namely, the elasticity, surface anchoring, and formation of the topological defects.[3,4] LCs exhibit long-range orientational ordering that underlie the existence of the elastic properties of the LCs. When the natural orientation of the LC medium is affected by an external or geometric constraint, deformation occur in their ordering that resulted in an energetic penalty, which can be approximated with $\sim KR$, where K is the Frank's elastic constant and R the sizescale, in the simplest form. When an LC medium is in contact with a surface, the interaction of the mesogenic molecules at the interface results in a preferred orientation of the LCs, called the easy axis. When the surface anchoring is perturbed away from the easy axis, an energetical penalty associated with this deformation occurs, which can be estimated as $\sim WR^2$, where W is the surface anchoring energy. When the LC medium can not satisfy the boundary conditions (surface anchoring) in the medium via just elastic deformations, topological defects occur within the medium, which are the local regions with broken LC symmetry. Overall, when the LCs are confined into microscopic volumes, they maintain a configuration which minimizes the free energy. Studies in the literature take advantage of such unique properties of LCs to synthesize materials with anisotropic optical, mechanical and responsive properties.[5–12]

Liquid crystals, when reactive, are shown to maintain their ordering after polymerization.[13,14] The two classes of polymeric materials that are synthesized using LC medium can be identified as liquid crystal elastomers and liquid crystal templated polymers. The mesogenic units in both of these classes of materials consists of reactive, polymerizable groups such as acrylates or epoxides.[15–20] Liquid crystal elastomers are the polymers that are usually synthesized from mixtures of mono- or di-functionalized reactive mesogenic units.[21,22] On the other hand, the so-called liquid crystal templated synthesis methods involve the use of the non-reactive mesogens along with reactive mesogens.[13,14] The difference of the use of non-reactive mesogens have been shown to provide additional control over the microstructure of the polymeric materials by providing aligned, mesoscopic pores, and three-dimensional shapes due to the anisotropic shrinkage after the removal of the unreacted part from the polymerized matrix.[13,18,23]

Liquid crystal templated synthesis of the particles has been shown to be advantageous over the synthesis using their isotropic counterparts. Past studies have demonstrated the use of techniques employing the emulsion polymerization, photolithography, and soft lithography for the synthesis of polymeric particles using nematic templates, which resulted in control over the surface morphologies, shape anisotropy, porosity and even chiral twisting of the particles.[13,18,19,24] However, although additional advantages are still present with the use of the cholesteric phase LC templates such as the structural coloring and three-dimensional ordering, minimal study has been reported on the use of CLCs in such synthesis applications.

In this study, we employ the use of CLCs in the templated synthesis of polymeric particles using microwells. We used sacrificial microwells of different shapes the provide the initial shapes to the particles. We chose to use circular, square, triangular and star shaped microwells analyze the effects of the confinement at different fundamental shape features. After polymerization, followed by the extraction of the unreacted part, we characterized the structure of the particles. We found that the elastic distortions within the particles would extent to a larger scale that would be expected from simple forms of the elastic distortions. We found that this is the result of the three-dimensional confinement, inhomogeneous surface anchoring and the cholesteric symmetry of the CLC templates.

2. Material and Method

2.1. Materials

A room temperature non-reactive nematic liquid crystal E7 (a commercial mixture of 51% of 4-cyano-4′-pentylbiphenyl (5CB), 25% of 4′-heptyl-4-biphenylcarbonitrile (7CB), 16% of 4′-n-octyloxy-4-cyanobiphenyl (8OCB) and 8% of 4-cyano-4″-n-pentyl-terphenyl (5CT)), a reactive mesogen 4-(3-acryloyoxy-propyloxy)benzoic acid 2-methyl-1,4-phenylene ester (RM257) and chiral dopant 4-((1-methylheptyloxycarbonyl)phenyl-4-hexyloxybenzoate) (S-811) were purchased from HCCH Jiangsu Hecheng Chemical Materials Co., Ltd. (Nanjing, China). Sylgard 184 silicon elastomer kit was obtained from Dow Corning. Octyltrichlorosilane (OTS), photoinitiator 2,2 dimethoxy-2-phenylacetophenone (DMPAP), polyvinyl alcohol (PVA), anhydrous acetone and, anhydrous toluene were obtained from Sigma-Aldrich Co. Ltd. (St. Louis, USA) and used without further treatment. Glass slides were obtained from Marienfeld GmbH (Lauda-Königshofen, Germany). Si wafers with microwells of different shapes prepared by deep reactive ion etching (DRIE) were obtained from METU MEMS Center. The depths of the features were measured to be around 11 μm.

2.2. Preparation of polyvinyl alcohol (PVA) molds

The preparation process was shown schematically in Figure 1A. Initially, the DRIE-processed Si wafers were coated with OTS with vapor deposition for 2 hours to maintain the adequate hydrophobicity for the soft lithography process. PDMS molds were prepared by initially mixing a pre-polymer-initiator ratio of 10:1. After well-mixing and de-gassing, the mixture was poured on the OTS-coated Si wafer and cured for 2 hours at 70°C. The PDMS molds were then peeled from the surface and used to prepare the PVA molds. 5% wt PVA was initially dissolved in ultrapure water until homogenous mixture was maintained. A large droplet of the PVA solution was placed on the PDMS-molds to cover and then dried overnight at room conditions. After drying, the PVA was peeled from the surface, and attached on a glass coverslip and used to synthesize the polymeric particles.

2.3. Preparation of the cholesteric liquid crystal templated polymeric particles

The particle synthesis procedure was shown schematically in Figure 1B. A reactive- and non-reactive mesogen mixture was prepared by mixing reactive mesogen RM257 (20%), photoinitiator DMPAP (1%), chiral dopant S811 (9%), and balance E7 by weight. Toluene was used as a co-solvent to dissolve and maintain a homogenous mixture and evaporated under vacuum to maintain a nematic mixture. 5 μL of the mesogen mixture was placed on the PVA mold that was previously attached to the glass substrates, and filled in the microwells using a spincoater (5 mins at 5000 rpm). After filling, the mixture was equilibrated for 30 min and polymerized with a 30 min exposure of UV light (365 nm) under vacuum. The polymerized particles present in the PVA microwells was cut and transferred into centrifuge tubes filled with water and mixed gently to dissolve PVA. To maintain a particle suspension free of PVA, the particles were centrifuged (5000 rpm, 5 mins) and the supernatant was replaced with fresh ultrapure water. This procedure was applied at least three times. Then, the centrifuge and the removal of the supernatant procedure was repeated with ethanol three times to remove the unreacted part of the particles. The particles were then dried under vacuum for further investigation.

2.4. Optical microscopy

An Olympus BX53 model microscope equipped with 4×, 10×, 50×, and 100× objectives and crossed polarizers were used for the optical characterization of the particles. The microscope is capable of imaging in transmission and reflection mode. Further image analyses and measurements were done using imageJ (NIH), an open source image analysis software.

2.5. Response measurements

For the measurements of the color change of the particles upon toluene vapor exposure, an in-house built exposure chamber with glass windows for imaging was used. Vacuum was maintained in the chamber with Edwards RV8 vacuum pump. Then, toluene was delivered in the system using a metering valve and its partial pressure was measured using a Baratron (MKS instruments) capacitance manometer with high precision. At each toluene concentration, the system was allowed to equilibrate for 5 minutes and images were collected. For each concentration, three independent particles were synthesized and three measurements from each batch was performed. The results were reported by calculating the average and standard deviation of the three independent measurements. The signals were reported using the formula;

$$Signal = [(R/G) - (R/G)_0 \ ]/(R/G)_0 \qquad \text{Eqn. 1}$$

where R and G represent the average intensities of the red and green signal measured from the particles in the reflection mode, and the subscript zero indicates their corresponding values before introduction of toluene into the system.

2.6. Electron Microscopy

Electron micrographs of the particles were collected using a Quanta 400F Field Emission series scanning electron microscope. The particles were dried on glass slides after the extraction of the reactive mesogens. Then, the samples were coated with gold with ion sputtering before electron microscopy imaging.

3. Results

The procedures we followed in the synthesis of the liquid crystal-templated microparticles consists of four major steps that affected the final structure of the particles. First, the reactive and non-reactive mesogen mixtures including a chiral dopant was prepared. The chiral dopant was present in the mixture to induce a chiral twist to the originally nematic mixture of E7 with RM257, thus resulted in a cholesteric phase. This mixture was then filled in PVA microwells (Figure 1B-C). The PVA surface was known to induce a planar alignment of the LCs, whereas the air (or vacuum) on the top side of the microwells is known to induce a homeotropic LC anchoring.[3,4,19] Thus, the mixtures were subjected to a hybrid surface anchoring conditions within the three-dimensional confinement maintained in the microwells. A result of this phenomena, the fingerprint textures, are evident in the CLCs filled within the microwells (Figure 1D). After polymerization of RM257 with UV light, we did not observe a major change in either the color and the fingerprint textures that indicated a minimal effect of the polymerization on the ordering within the particles. After polymerization, we dissolved the PVA microwell in water and obtained the free particles. Lastly, the particles were treated with ethanol to extract the unreacted part. After extraction, the particles shrunk and maintained their final shapes and structure. When the optical appearance of the particles obtained were compared with those of the just polymerized particles, we observed a difference in their coloring. Apparently, the particles after the extraction step exhibited a reflection of color in the visible light wavelengths (mostly green), which is an outcome of the Bragg reflections due to the periodic cholesteric structure. The reason of the appearance of the Bragg reflections in the final state but not in the previous steps were due to the larger periodicity of the cholesteric phase observed for 9% wt S811 doped mixtures. However, after extraction of the unreacted part leading to shrinkage, the particles maintained a periodic structure that can interact with visible light and exhibit Bragg reflections within the visible light wavelengths. For such concentrations, we have characterized the shrinkage of the polymeric matrix in the direction of the cholesteric axis to be ~45%.[23] Thus, the larger pitch size of the CLC maintained initially (larger than the wavelengths corresponding to those of the visible light) was reasonable.
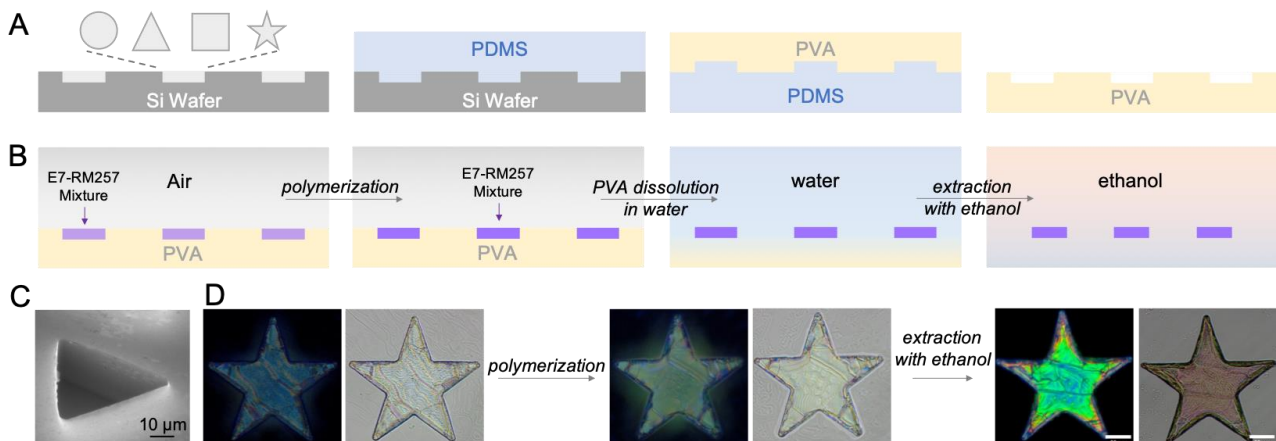

Figure 1. Experimental procedures for the synthesis of cholesteric liquid crystal-templated synthesis of polymeric particles using microwells. (A) sketch of the procedures for the preparation of sacrificial PVA microwells. (B) Sketch of the procedures followed for the synthesis of microparticles. (C) Electron micrograph of a triangle shaped PVA microwell of size 50 μm. the microwell is imaged with a tilt, showing the perpendicular walls of the wells. (D) Representative micrographs of the star shaped particles synthesized from 9% wt S811, 20% wt RM257, 1% DMPAP and balance E7. Reflection-mode polarized light (left) and brightfield (right) micrographs are shown.
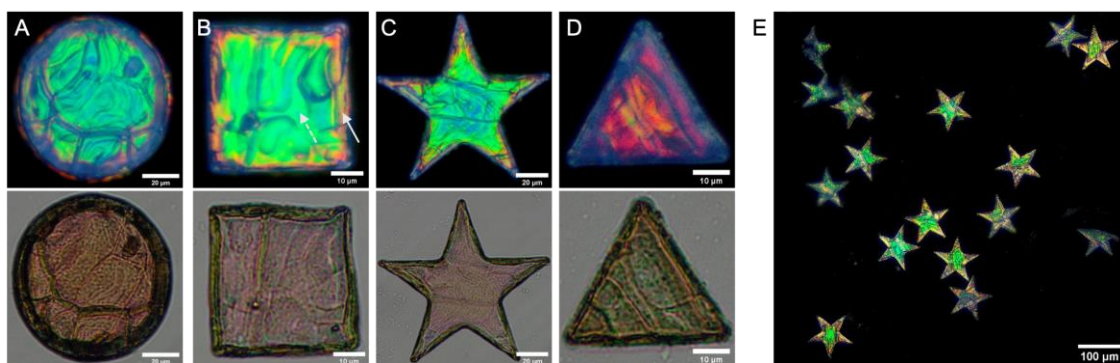
Figure 2. Representative micrographs of (A) circle, (B) square, (C) star, and (D) triangle shaped particles synthesized from 9% wt S811, 20% wt RM257, 1% DMPAP and balance E7 using microwells. Reflection-mode polarized light (top row) and brightfield (bottom row) micrographs are shown. (E) A larger area micrograph of particles synthesized from the same batch showing monodispersity.

When the optical micrographs of the particles were compared, we observed that the majority of the particles maintained a bright, green color that is consistent with the expected Bragg reflection from the particles synthesized from this composition. However, there are two features that are important to highlight. First, when carefully investigated, the sides of each particle are evidently reflecting colors in red, in some places even did not reflect color in the visible wavelengths. Given that the microwells maintained shapes that were sharp and perpendicular intersections at the edges (Figure 1C), we reasoned that the different colorings at the edges of the particles were due to the three-dimensional confinement of the particles. Specifically, the particles were synthesized from LC medium that mediated planar anchoring at their contact with the PVA surface and homeotropic anchoring at their contact with air (or vacuum). Due to this inhomogenous anchoring, a significant elastic distortion was expected at the edges of the particles. If this is the case, the size scale expected from the distortions that result from the interplay of elastic energy (that scales with $\sim KR$, where K is the Frank's Elastic constant, typically in the order of 10^{-11} J/m, and R the size scale) and surface anchoring energy (that scales with $\sim WR^2$, where W is the surface anchoring energy, typically in the order of 10^{-6} J/m^2) is ~ 10 μm. Consistent with this estimation, we measured the thickness of the sides of the particles where we observed a different coloring to be 7 ± 2 μm, which supports the effect of the elastic contributions to the internal configuration of LCs initially maintained in the microwells. Due to this elastic distortion, the particles did not exhibit significant shrinkage at the regions close to the sides that resulted in the reflection of colors at higher wavelengths. Consistent with this effect, we observed that such coloring to be maintained in the majority of the square shaped particles. Although the triangle shaped particles were in the sizes of 50 μm by side, they did not exhibit significant shrinkage as compared to the particles synthesized from different shaped microwells. This was due to the narrow edges of the particles that were making 60° with each side. Thus, the elastic distortions within the LC matrix were amplified to affect the larger volumes within the microwells.

Here we also note that such reduction in the shrinkage was observed in the particles along their radial dimension. When the shrinkage of the circular shaped particles with 100, 50 and 7 μm in sizes were measured, we found a reduction in the shrinkage from 10.5 ± 1.8 μm, 8.8 ± 1.4 μm to 7.7 ± 2.5 μm, for 100, 50 and 7 μm particles, respectively (Figure 3). Although not in the same direction that resulted in the reflection of color in the visible light wavelengths, the effects of confinement were also reflected in the shrinkage of the particles.
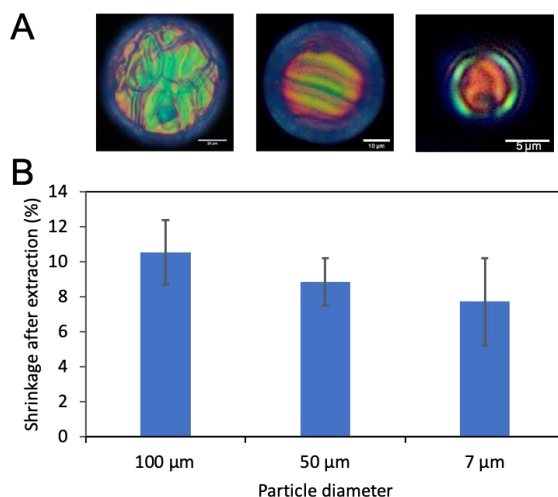
Figure 3. (A) Reflection mode polarized optical micrographs of different shaped particles synthesized from in 9% wt S811, 20% wt RM257, 1% DMPAP and balance E7 circular shaped microwells. (B) Per cent shrinkage of the particles after extraction of the unreacted mesogens as a function of size. The mesurements were done fro mthe optical images.

Next, scanning electron micrographs of the particles were collected to characterize the structure of the particles synthesized from CLC templates using different microwell shapes (Figure 4A). Consistent with the optical microscopy images, we observed flat shaped appearance of the particles. When compared with the particles synthesized from the nematic shaped particles with the same, inhomogenous surface anchoring, the formation of the flat shaped particles from cholesteric templates were interesting. It was shown in previous studies that the particles curl when there is a non-parallel surface anchoring of LCs at the two opposite sides of the particles.[18,19,24] This was shown to result from the imbalance in the shrinkages of the two sides of the particles after the extraction of the unreacted mesogens.[19] Although a similar, non-parallel surface anchoring of LC at the two opposite sides was maintained here, we did not observe the particles to curl, independent of the overall shapes of the particles. This is due to the internal cholesteric symmetry of the mesogens maintained in the particles. Due to the cholesteric configuration with cholesteric axis perpendicular to the bottom side of the particles, they did not shrink anisotropically, thus, resulted in the isotropic shrinkage of the particles after extraction of the unreacted part. This effect also resulted in the formation of the particles with bright appearance after shrinkage. In addition to the overall shapes of the particles, we also observed that the surface morphology of the particles was consistent with the cholesteric twist that resulted in the twisted surface morphology of the particles (Figure 4B).
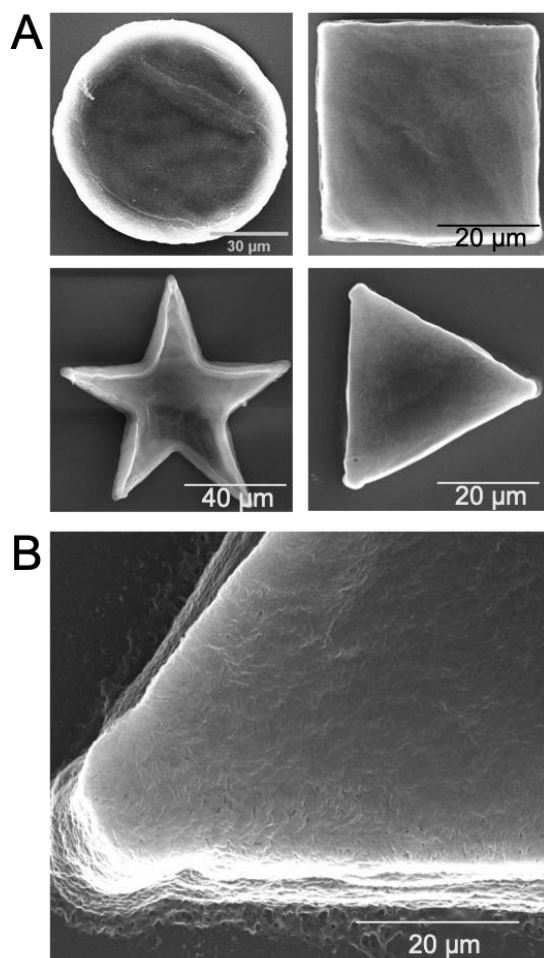
Figure 4. (A) Scanning electron micrographs of different shaped particles. (B) Scanning electron micrograph of a triangle shaped particle showing the surface features. Particles were synthesized from in 9% wt S811, 20% wt RM257, 1% DMPAP and balance E7.

In the last set of experiments, we measured the response of the particles against the presence of toluene vapor in the system. For this, we placed a population of particles in a chamber where the toluene vapor concentration was controlled and collected their micrographs. Representative images of an experiment collected with square shaped particles are shown in Figure 5. As shown in the images, upon exposure to toluene vapor, the color appearance of the particles was shifted to higher wavelengths. At the end, when the system was evacuated from toluene, the color appearance of the particles was recovered back to their initial state, showing their reversibility.
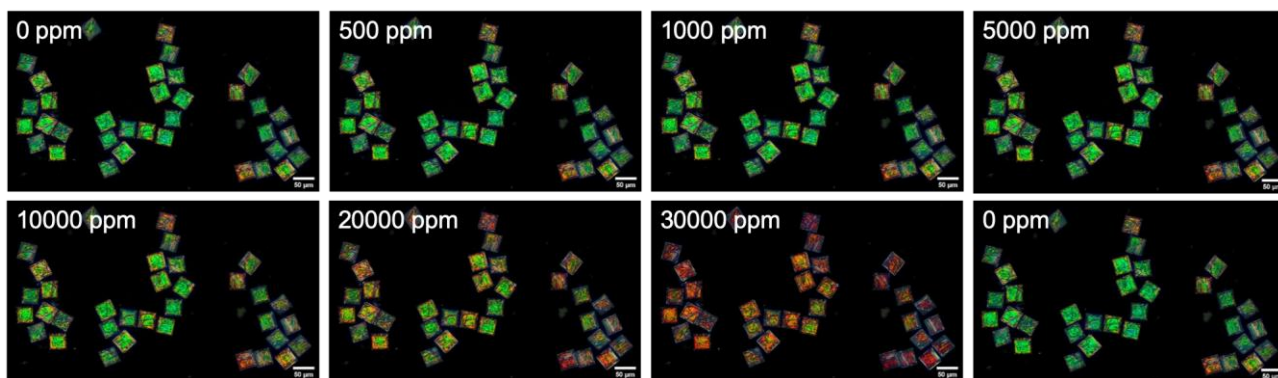

Figure 5. Reflection mode optical micrographs of particles collected upon exposure to toluene vapor. Particles were synthesized from in 9% wt S811, 20% wt RM257, 1% DMPAP and balance E7. The values on the top left of each image indicate the concentration of exposed toluene. The last micrograph shows the optical appearance of the particles after removal of toluene from the exposure chamber.

To collect statistical information, we have repeated the response measurements of the particles from three independent measurements and analyzed the appearance of the particles by their RGB color change as function for toluene concentration using the signal formula described in the experimental section. The averages and the standard deviation of these experiments were reported in Figure 6. When the three response curves were compared, the difference between the response of the triangular shaped particles is apparent. Specifically, the response of the star and square shaped particles exhibited a response with two trends, from 0 ppm to 1000 ppm with one slope, from 1000 to 5000 ppm with a lower slope, whereas the response of the triangle shaped particles exhibited a monotonous response against increasing toluene concentration. More importantly, although the particles were synthesized from the same cholesteric liquid crystal compositions, this set of data showed that the shapes of the particles to play a critical role in the response of the particles. Past studies on the measurements of such particles showed that the two-trend response of the particles to result from the elastic energy stored within the particles upon shrinkage after the extraction of the unreacted mesogens.[25] Thus, when combined with the red appearance of the triangular shaped particles under polarized microscope described above, the loss of the sensitivity for the triangular shaped particles compared to the other shapes can be concluded to be the absence of significant shrinkage, therefore the absence of the elastic energy storage within the particles. This observation, then highlights the importance of the particle shapes, in addition to the size effects shown in the previous studies.[25]
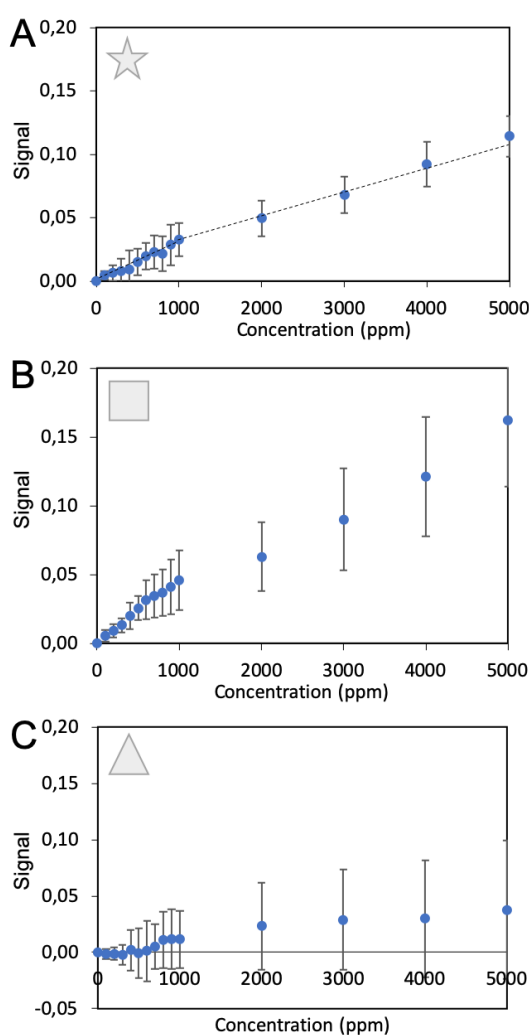

Figure 6. Response curves of the (A) star, (B) square, and (C) triangle shaped particles collected upon exposure to toluene vapor. Particles were synthesized from in 9% wt S811, 20% wt RM257, 1% DMPAP and balance E7. The measurements were performed upon increasing the toluene concentration. Three independent response measurements were performed for each set of data, the averages and standart measurements were calculated.

4. Discussion and Conclusion

The study reported in this article demonstrates the effect of shape, in addition to the size as shown in previous studies, on the response and sensitivity of the particles upon exposure to toluene vapor. The study herein

highlights the importance of the shape that needs to be considered when designing sensor materials using liquid crystals as molecular templates. Although the liquid crystal templated synthesis methods provide easy means provide additional response to the sensors through the elasticity, it was shown in this study that the three dimensional shapes of the particles are needed to be considered in more detail. Otherwise, the shapes with narrow edges that provide a complicated three dimensional LC director profiles that would prevent shrinkage required for the storage of the elastic energy, which provided the additional response to the sensors. The findings of this study will be used in further developments of the analytical methods based on optically active polymeric materials, to provide higher sensitivity with no additional cost of supplied energy.

Acknowledgment

References

[1] de Gennes, P. G., Prost, J. 1993. The Physics of Liquid Crystals. 2nd edition. Oxford, New York.

[2] White, T. J., McConney, M. E., Bunning, T. J. 2010. Dynamic Color in Stimuli-Responsive Cholesteric Liquid Crystals. Journal of Materials Chemistry, 20, 9832–9847,

[3] Bukusoglu, E., Bedolla-Pantoja, M. A., Mushenheim, P. C., Wang, X., Abbott, N. L. 2016. Design of Responsive and Active (Soft) Materials Using Liquid Crystals. Annual Review in Chemical and Biomolecular Engineering, 7, 163–196.

[4] Bai, Y., Abbott, N. L. 2011. Recent Advances in Colloidal and Interfacial Phenomena Involving Liquid Crystals. Langmuir, 27, 5719–5738.

[5] Herzer, N., Guneysu, H., Davies, D. J. D., Yildirim, D., Vaccaro, A. R., Broer, D. J., Bastiaansen, C. W. M., Schenning, A. P. H. J. 2012. Printable Optical Sensors Based on H-bonded Supramolecular Cholesteric Liquid Crystal Networks. Journal of American Chemical Society, 134, 7608–7611.

[6] Han, Y., Pacheco, K., Bastiaansen, C. W. M., Broer, D. J., Sijbesma, R. P. 2010. Optical Monitoring of Gases with Cholesteric Liquid Crystals. Journal of American Chemical Society, 132, 2961–2967.

[7] Sutarlie, L., Qin, H., Yang, K. L. 2010. Polymer Stabilized Cholesteric Liquid Crystal Arrays for Detecting Vaporous Amines. Analyst, 135, 1691–1696.

[8] Iamsaard, S., Aßhoff, S. J., Matt, B., Kudernac, T., Cornelissen, J. J. L. M., Fletcher, S. P., Katsonis, N. 2014. Conversion of Light into Macroscopic Helical Motion. Nature Chemistry, 6, 229–235.

[9] Gelebart, A. H., Liu, D., Mulder, D. J., Leunissen, K. H. J., van Gerven, J., Schenning, A. P. H. J., Broer, D. J. 2018. Photoresponsive Sponge-Like Coating for On-Demand Liquid Release. Advanced Functional Materials, 28, 1705942.

[10] Kotikian, A., Truby, R. L., Boley, J. W., White, T. J., Lewis, J. A. 2018. 3D Printing of Liquid Crystal Elastomeric Actuators with Spatially Programed Nematic Order. Advanced Materials, 30, 1–6.

[11] Feng, W., Broer, D. J., Liu, D. 2018. Oscillating Chiral-Nematic Fingerprints Wipe Away Dust. Advanced Materials, 1704970, 1704970.

[12] White, T. J., Broer, D. J. 2015. Programmable and Adaptive Mechanics with Liquid Crystal Polymer Networks and Elastomers. Nature Materials, 14, 1087–1098.

[13] Wang, X., Bukusoglu, E., Miller, D. S., Bedolla-Pantoja, M. A., Xiang, J., Lavrentovich, O. D., Abbott, N. L. 2016. Synthesis of Optically Complex, Porous, and Anisometric Polymeric Microparticles by Templating from Liquid Crystalline Droplets. Advanced Functional Materials, 26, 7343–7351.

[14] Mondiot, F., Wang, X., de Pablo, J. J., Abbott, N. L. 2013. Liquid Crystal-Based Emulsions for Synthesis of Spherical and Non- Spherical Particles with Chemical Patches. Journal of the American Chemical Society, 135, 9972–9975.

[15] Li, Y., Pruitt, C., Rios, O., Wei, L., Rock, M., Keum, J. K., Mcdonald, A. G., Kessler, M. R. 2015. Controlled Shape Memory Behavior of a Smectic Main-Chain Liquid Crystalline Elastomer. Macromolecules, 48, 2864–2874.

[16] Petsch, S., Rix, R., Khatri, B., Schuhladen, S., Müller, P., Zentel, R., Zappe, H. 2015. Smart Artificial mMuscle Actuators: Liquid Crystal Elastomers with Integrated Temperature Feedback. Sensors and Actuators, A: Physical, 231, 44–51.

[17] Fleischmann, E. K., Liang, H. L., Kapernaum, N., Giesselmann, F., Lagerwall, J., Zentel, R. 2012. One-Piece Micropumps from Liquid Crystalline Core-Shell Particles. Nature Communications, 3, 1178.

[18] Karausta, A., Bukusoglu, E. 2018. Liquid Crystal-Templated Synthesis of Mesoporous Membranes with Predetermined Pore Alignment. ACS Applied Materials and Interfaces, 10, 33484–33492.

[19] Akdeniz, B., Bukusoglu, E. 2019. Design Parameters and Principles of Liquid-Crystal-Templated Synthesis of Polymeric Materials via Photolithography. Langmuir, 35, 13126–13134.

[20] De Haan, L. T., Sánchez-Somolinos, C., Bastiaansen, C. M. W., Schenning, A. P. H. J., Broer, D. J. 2012. Engineering of Complex Order and the Macroscopic Deformation of Liquid Crystal Polymer Networks. Angewandte Chemie - International Edition, 51, 12469–12472.

[21] White, T. J., Serak, S. V., Tabiryan, N. V., Vaia, R. A., Bunning, T. J. 2009. Polarization-Controlled, Photodriven Bending in Monodomain Liquid Crystal Elastomer Cantilevers. Journal of Materials Chemistry, 19, 1080–1085.

[22] Sawa, Y., Ye, F., Urayama, K., Takigawa, T., Gimenez-Pinto, V., Selinger, R. L. B., Selinger, J. V. 2011. Shape Selection of Twist-Nematic-Elastomer Ribbons. Proceedings of the National Academy of the Sciences of the USA, 108, 6364–6368.

[23] Batir, O., Bat, E., Bukusoglu, E. 2020. Strain-Enhanced Sensitivity of Polymeric Sensors Templated from Cholesteric Liquid Crystals. Soft Matter, 16, 6794–6802.

[24] Akdeniz, B., Bukusoglu, E. 2019. Liquid Crystal Templates Combined with Photolithography Enable Synthesis of Chiral Twisted Polymeric Microparticles. Macromolecular Rapid Communications, 40, 1900160.

[25] Avşar, D. I., Bukusoglu, E. 2020. Chameleon Skin-Inspired Polymeric Particles for the Detection of Toluene Vapor. Soft Matter, 16, 8683–8691.